Synthesis of visible-light-responsive $YbTaO_{4-x}N_y$ via work-function-difference metal assistance nitridation for photocatalytic overall water splitting

Hai Zou,[a] Xueshang Xin,[b] & Fuxiang Zhang[b]*

[a] *College of Chemistry and Chemical Engineering, Chongqing University of Science and Technology, Chongqing 401331, P. R. China*

[b] *State Key Laboratory of Catalysis, Dalian National Laboratory for Clean Energy, Dalian Institute of Chemical Physics, Chinese Academy of Sciences, Zhongshan Road 457, Dalian, 116023, China. Email: fxzhang@dicp.ac.cn*

*Corresponding Author

E-mail: fxzhang@dicp.ac.cn.

1. Experimental

Chemical Reagents.

Ytterbium oxide (Yb_2O_3, 99.9%), magnesium powder (Mg, 99.5%), zirconium powder (Zr, 99.5%), aluminium powder (Al, AR) and anhydrous sodium sulfate (Na_2SO_4, AR) were purchased from Aladdin Reagent Co., Ltd. Tantalum oxide (Ta_2O_5, 99.99%) was supplied by High Purity Chemicals, Japan. Potassium chloride (KCl, ≥ 99.8%), hexachloroiridic acid hexahydrate ($H_2IrCl_6 \cdot 6\ H_2O$, Ir basis ≥ 39%) and bismuth nitrate pentahydrate ($Bi(NO_3)_3 \cdot 5H_2O$, AR) were obtained from Macklin Biochemical Co., Ltd. Potassium ferrocyanide ($K_4[Fe(CN)_6]$, AR) was obtained from Alfa Aesar. Ammonium metavanadate (NH_4VO_3, AR), hexachloroplatinic acid hexahydrate ($H_2PtCl_6 \cdot 6\ H_2O$, Pt basis ≥ 37%), potassium chromate (K_2CrO_4, 99.5%), sodium hydroxide (NaOH, AR), absolute ethanol (C_2H_5OH, ≥ 99.7%), methanol (CH_3OH, ≥ 99.5%), concentrated hydrochloric acid (HCl, 36–38%), concentrated nitric acid (HNO_3, 65%) and potassium ferrocyanide ($K_4[Fe(CN)_6]$, 99.5%) were provided by Sinopharm Chemical Reagent Co., Ltd.

Materials Synthesis

Firstly, the $YbTaO_4$ was prepared by a KCl-flux method adapted from previous report.[1] A mixture of 788 mg Yb_2O_5, 884 mg Ta_2O_5 and 1672 mg KCl was ground in an agate mortar for 30 min. After mixed thoroughly, it was transferred to a 50 mL alumina crucible, heated in a muffle furnace to 1423 K at 10 K min^{-1}, held for 5 h. When cooling down, it was stirred in 200 mL deionized water at 353 K to dissolve the flux, filtered, washed and dried at 333 K overnight, yielding $YbTaO_4$ powder.

Nitridation was performed in a horizontal tube furnace under 250 mL min^{-1} anhydrous NH_3. For the synthesis of $YbTaO_{4-x}N_y$(Mg), 0.5 g $YbTaO_4$ and 0.25 g Mg powder were mixed and loaded into an alumina boat, then it was heated from ambient to 923 K at 10 K min^{-1}, maintained for 10 h in a tube furnace with NH_3 flow. Analogous procedures were used for $YbTaO_{4-x}N_y$(Zr) and $YbTaO_{4-x}N_y$(Al) by replacing Mg with Zr or Al powder. $YbTaO_{4-x}N_y$ was prepared identically but without any metal additive. After nitridation, residual metals and their derivative were removed by stirring in 1 M HNO_3 for Mg powder, 1 M KOH for Al powder, or ultrasonic dispersion and sedimentation for Zr powder. The powders were then rinsed to neutral pH and dried at 333 K overnight.

Loading of Cocatalyst

For H_2-evolution half-reaction, Pt nanoparticles were deposited as a cocatalyst via classical wet impregnation followed by H_2 reduction. Typically, 200 mg of photocatalyst powder was ultrasonically dispersed in 2 mL of H_2PtCl_6 solution containing the calculated Pt amount. The slurry was dried in a 353 K water bath, transferred to a tube furnace, and reduced at 473 K for 1 h under 5% H_2/95% Ar (*vol.*/*vol.*). After cooling, the powder was collected. For Z-scheme overall water splitting, the oxygen-evolution component Ir-$FeCoO_x$/$BiVO_4$ was prepared as the previous literature reported.[2] For one-step overall water splitting, Pt and IrO_2 served as H_2 and O_2-evolution co-catalysts, respectively. And CrO_x was photodeposited on Pt nanoparticles to prevent the reverse reaction of water splitting. After Pt loaded, the photocatalyst was ultrasonically dispersed in 20 *vol*.% aqueous methanol containing 1 *wt*.% K_2CrO_4 (calculated as Cr content). The suspension was evacuated and illuminated with a 300 W Xe lamp ($\lambda \geq 420$ nm) for 3 h, then filtered, washed, and dried. IrO_2 sol was subsequently loaded by adsorption, the Pt@CrO_x-loaded powder was dispersed in 20 mL of IrO_2 sol with predetermined concentration, stirred for 6 h, filtered, washed, and air-dried. The IrO_2 sol was prepared according previous reported,[3] 5 mL of 1 mg mL^{-1} H_2IrCl_6 solution was diluted to 100 mL with water, adjusted to pH 12 with 1 M KOH, and heated at 353 K for 0.5 h until colorless. After ice-bath cooling to room temperature, the pH was re-adjusted to 9 with 1 M HCl and the solution was heated again at 353 K for 1 h, yielding a deep-blue IrO_2 sol.

Characterization

Powder X-ray diffraction pattern (XRD) measurement was carried out on a SmartLab X-ray diffractometer (Cu Kα radiation, λ = 1.5418 Å). And the Rietveld refinement for XRD was performed on a General Structure Analysis System (GSAS) software.[4] The morphology and size were observed by a JSM-7900F field emission scanning electron microscope (SEM) and energy dispersive X-Ray Spectroscopy (EDS). UV-vis diffuse reflectance spectroscopy (UV-vis DRS) was obtained on a Shimadzu UV2600 with $BaSO_4$ as background. The Tauc plot was constructed from the UV-Vis DRS data in accordance with the following equation: $(\alpha h\nu) = A(h\nu - E_g)^n$. Herein, α denotes the absorption coefficient, which was approximated by the Kubelka-Munk function F(R), hν represents the photon energy, A is a constant irrelevant to photon energy, n is set to 2 for indirect allowed transitions, E_g stands for the band gap energy of the sample, and F(R) is the Kubelka-Munk function calculated by the formula $F(R) = (1-R)^2/(2R)$, where R refers to the reflectance of an infinitely thick sample. Subsequently, the Tauc plot was generated by plotting $(F(R)h\nu)^{1/2}$

against hν, and the band gap energy E_g was determined by extrapolating the linear segment of the plot to the point where $(F(R)h\nu)^{1/2} = 0$. Thermogravimetric analysis was conducted on a PerkinElmer Diamond TG/DTA analyzer in an air atmosphere. The open-circuit voltage measurements were performed on a Solartron electrochemical workstation in 0.1 M Na_2SO_4 solution. Time-resolved photoluminescence (TRPL) decay spectra were measured using an Edinburgh FLS1000 fluorescence spectrometer, with excitation by a 375 nm pulsed laser. Ultraviolet photoelectron spectroscopy (UPS) measurements were performed on a Shimadzu AXIS SUPRA+ spectrometer. Prior to each test, the sample was etched with argon ions for 2 minutes to eliminate surface contaminants. The working function (Φ) was calculated using the equation that $\Phi = h\nu - (E_{cutoff} - E_{Feimi})$, where *hv* is the photon energy of the He I source (21.22 eV), and the cutoff binding energy (E_{cutoff}) and Fermi binding energy (E_{Feimi}) were derived from the midpoint of the secondary electron cutoff and the onset of the Fermi edge.

Photocatalytic Performance

The photocatalytic activity was tested on a Pyrex top-illuminated reactor with a 288 K reflux condensing unit wrapped. For proton reduction half-reaction, 100 mg photocatalyst loaded with calculated Pt was ultrasonically dispersed in 20 *vol*.% CH_3OH. For Z-scheme overall water splitting, 100 mg H_2-evolving photocatalyst loaded with calculated Pt and 50 mg Ir-$FeCoO_x$/$BiVO_4$ were ultrasonically dispersed in 150 mL phosphate buffer solution (PBS, pH=6, 25 mM) containing 5 mM $K_4[Fe(CN)_6]$.[2] For one step photocatalytic overall water splitting, 100 mg photocatalyst loaded with Pt@CrO_x and IrO_2 was ultrasonically dispersed in 150 mL H_2O. Before each test, the air was completely removed by pumping for 30 min. The light source comes from a 300 W Xenon lamp with a filter to cut off ultraviolet light ($\lambda \geq 420$ nm). A gas chromatography (GC-2014, Shimadzu) connected to the photocatalyst reactor was utilized to detect the type and the cumulative amount of gases evolved.

Mott-Schottky test

The Mott-Schottky test was carried out on a Princeton electrochemical workstation. For the preparation of the working electrode, sample powder of 10 mg was dispersed in 1 mL ethanol with 10 μL 5 *wt.*% nafion solution, drop it on a piece of 1×2 cm^2 fluorine-doped tin oxide (FTO) glass. After that, the edge of the FTO glass was covered by glue. A Pt sheet and an Ag/AgCl electrode were employed as a counter electrode and a reference electrode, respectively. The electrolyte is 0.5 M Na_2SO_4 solution. The measured potential was converted into the reversible hydrogen

electrode (RHE) reference via the Nernst equation, expressed as E(*vs*. RHE) = E(*vs*. Ag/AgCl) + 0.197 + 0.0591 × pH, where the pH value was fixed at 7.

2. Results

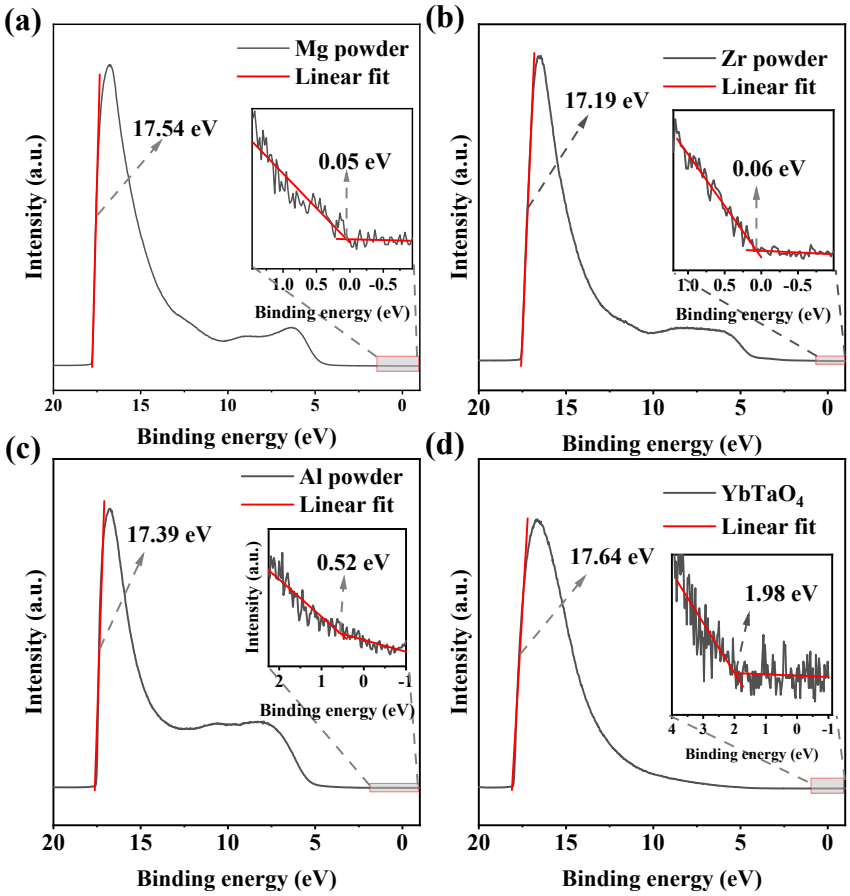

Fig. S1 UPS of (a) $YbTaO_{4-x}N_y$(Mg), (b) $YbTaO_{4-x}N_y$(Zr), (c) $YbTaO_{4-x}N_y$(Al), and (d) $YbTaO_4$.

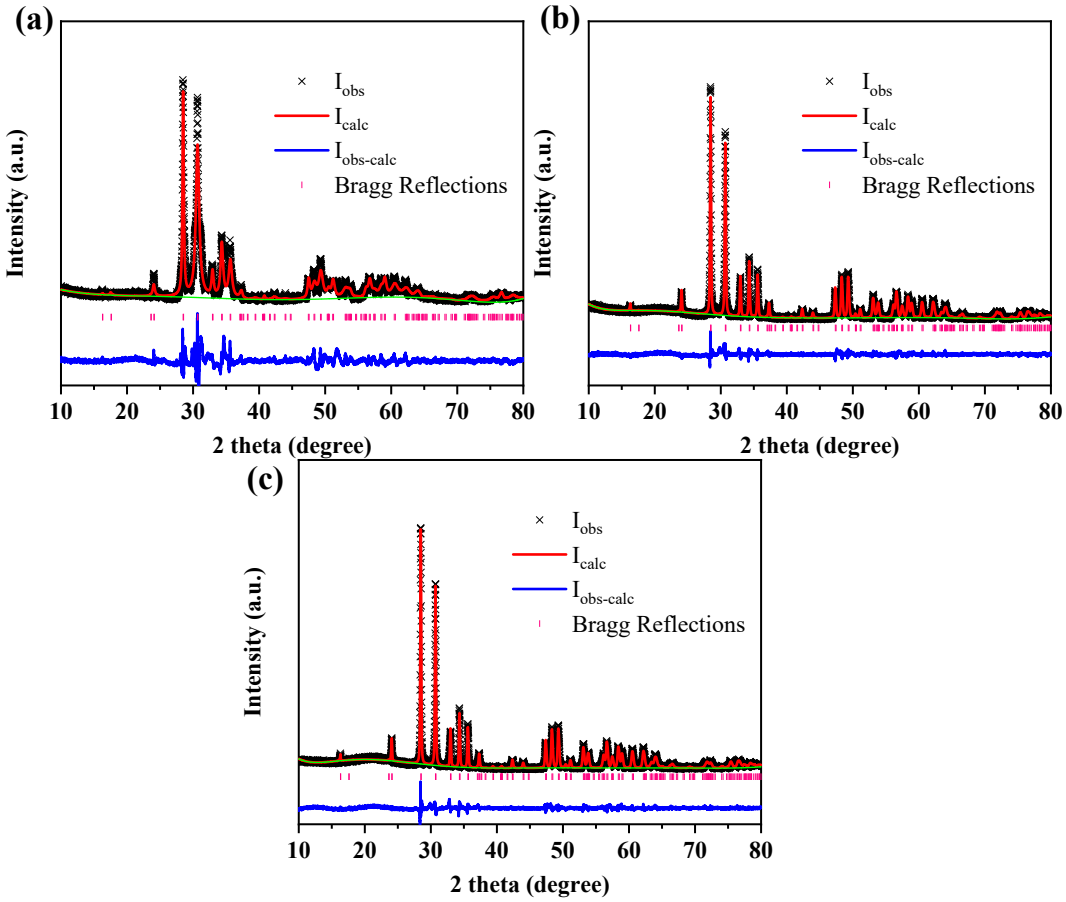

Fig. S2 Rietveld refinement results of (a) $YbTaO_{4-x}N_y$(Zr), (b) $YbTaO_{4-x}N_y$(Al) and (c) $YbTaO_{4-x}N_y$.

Table S1 Cell parameters of samples obtained from Rietveld refinement.

Samples	a (nm)	b (nm)	c (nm)	α	β	γ	R_p	R_{wp}	χ^2
$YbTaO_{4-x}N_y$(Mg)	5.2490	5.4357	5.0603	90º	96.06 º	90º	7.58%	10.43%	6.20
$YbTaO_{4-x}N_y$(Zr)	5.2486	5.4355	5.0652	90º	95.85º	90º	8.06%	10.70%	6.83
$YbTaO_{4-x}N_y$(Al)	5.2522	5.4309	5.0690	90º	96.09º	90º	5.52%	7.16%	2.19
$YbTaO_{4-x}N_y$	5.2498	5.4286	5.0674	90º	96.09º	90º	5.79%	7.58%	2.70

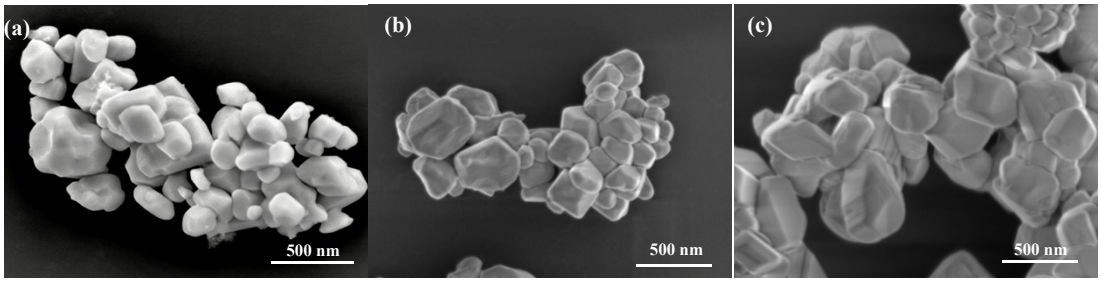

Fig. S3 SEM images of (a) $YbTaO_{4-x}N_y$(Zr), (b) $YbTaO_{4-x}N_y$(Al) and (c) $YbTaO_{4-x}N_y$.

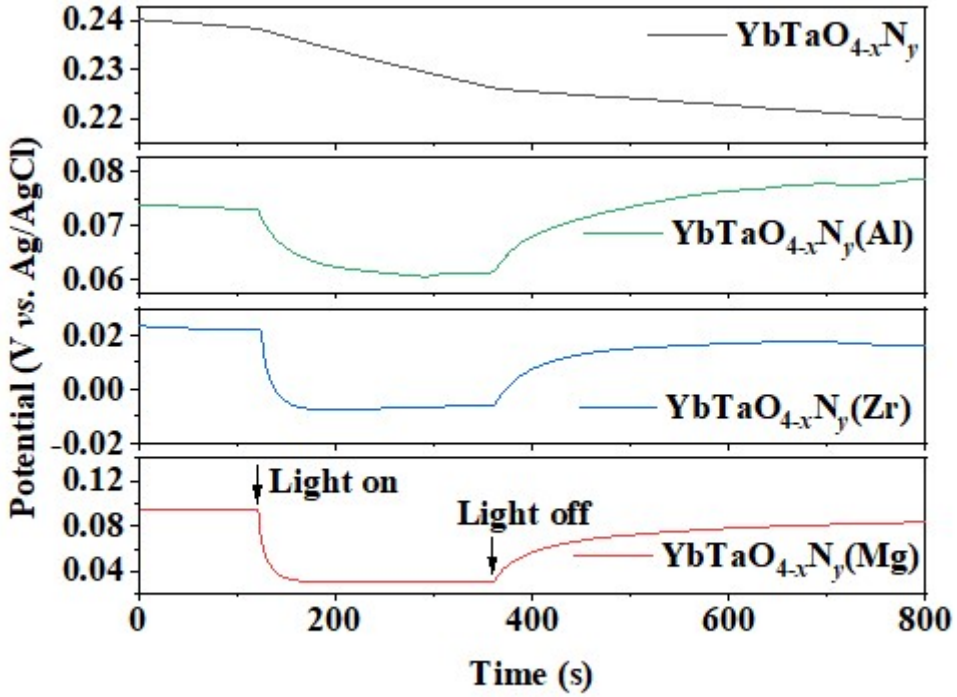

Fig. S4 Open-circuit potential of nitride samples under dark state and light switching.

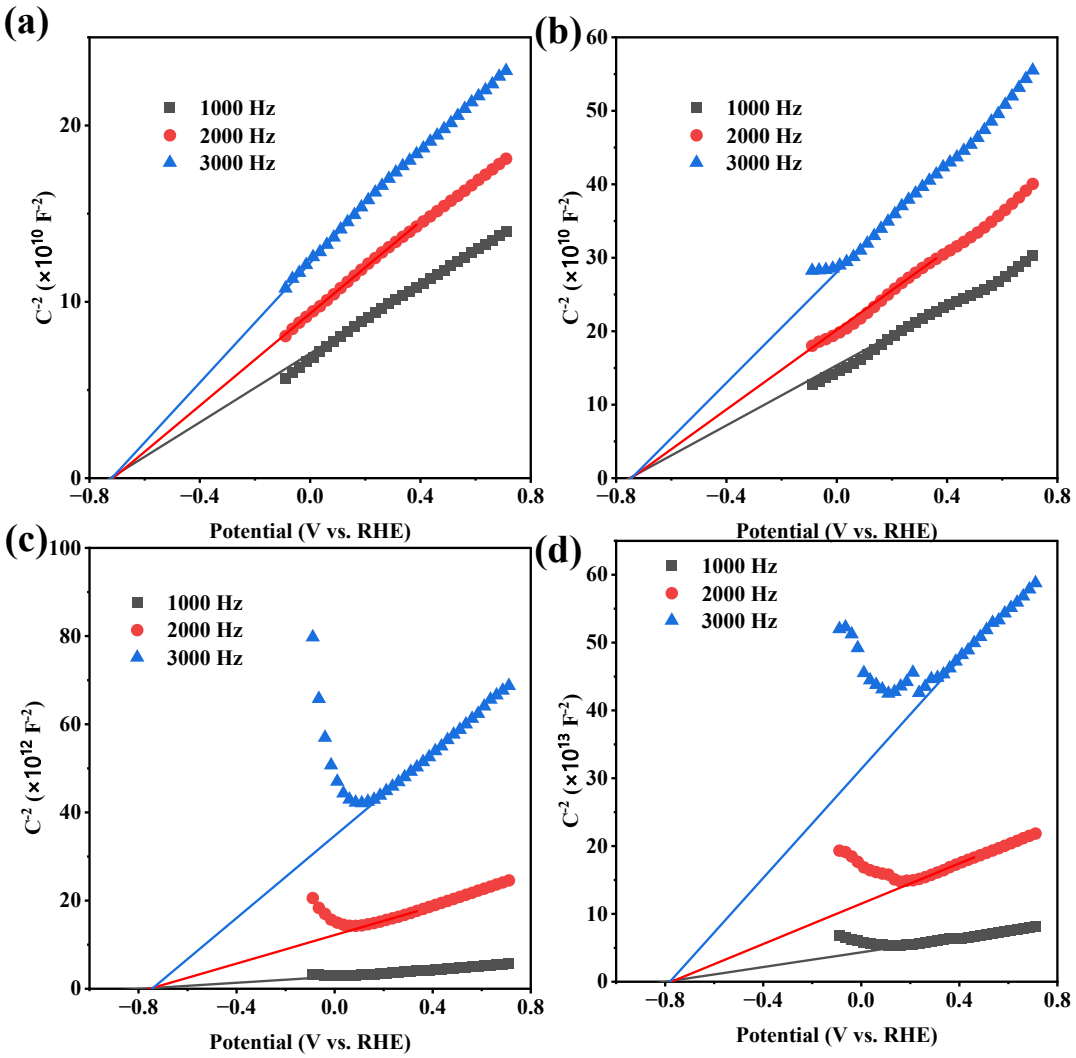

Fig. S5 Mott-Schottky plots of (a) $YbTaO_{4-x}N_y$(Zr), (b) $YbTaO_{4-x}N_y$(Al), (c) $YbTaO_{4-x}N_y$, and (d) $YbTaO_4$ at different frequencies.

The Mott-Schottky measurement was carried out in 0.5 M Na_2SO_4 and the measured potential (E *vs*. Ag/AgCl) was converted into the potential versus reversible hydrogen electrode (RHE) by E(*vs*. RHE) = E (*vs*. Ag/AgCl) + 0.197 + 0.0591 × 7.

Table S2 Band structure parameters of samples.

Samples	E_g (eV)	CB (eV)	VB (eV)[a]
$YbTaO_{4-x}N_y$(Mg)	2.3	-0.8	1.5
$YbTaO_{4-x}N_y$(Zr)	2.6	-0.8	1.8
$YbTaO_{4-x}N_y$(Al)	2.8	-0.9	1.9
$YbTaO_{4-x}N_y$	3.8	-0.9	2.9
$YbTaO_4$	4.0	-0.9	3.1

[a] Valence band (VB) was calculated by the formula that VB = E_g + CB.

Table S3 Fitting parameters of TRPL by double exponential decay

Sample	τ_1 (ns) [a]	f_1 [b]	τ_2 (ns) [a]	f_2 [b]	τ_{ave}(ns) [c]
$YbTaO_{4-x}N_y$(Mg)	1.42	71.2%	7.32	28.8%	3.12
$YbTaO_{4-x}N_y$(Zr)	1.38	65.6%	6.46	34.4%	3.13
$YbTaO_{4-x}N_y$(Al)	0.92	66.6%	5.42	33.4%	2.42
$YbTaO_{4-x}N_y$	0.69	78.7%	4.17	21.3%	1.43

[a] τ_1 and τ_2 are the carrier lifetimes.

[b] f_1 and f_2 are the fractional intensities.

[c] τ_{ave} is the intensity-weighted average lifetime, which is equal to $f1\tau_1 + f_2\tau_2$.

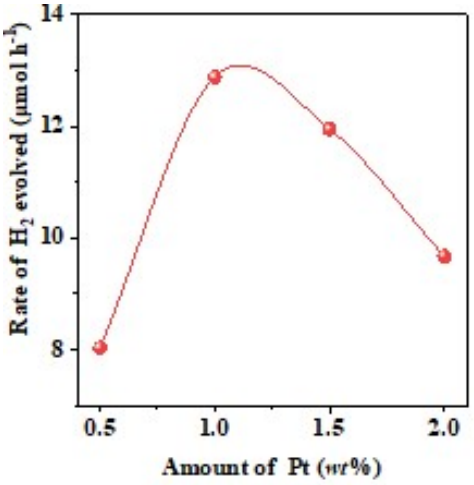

Fig. S6 Optimization curve of Pt cocatalyst content loading on $YbTaO_{4-x}N_y$(Mg) for hydrogen evolution reaction.

Reaction conditions: 100 mg Pt/$YbTaO_{4-x}N_y$(Mg), 150 mL 20 *vol*.% methanol solution, 300 W Xe lamp with a cutoff filter ($\lambda \geq 420$ nm).

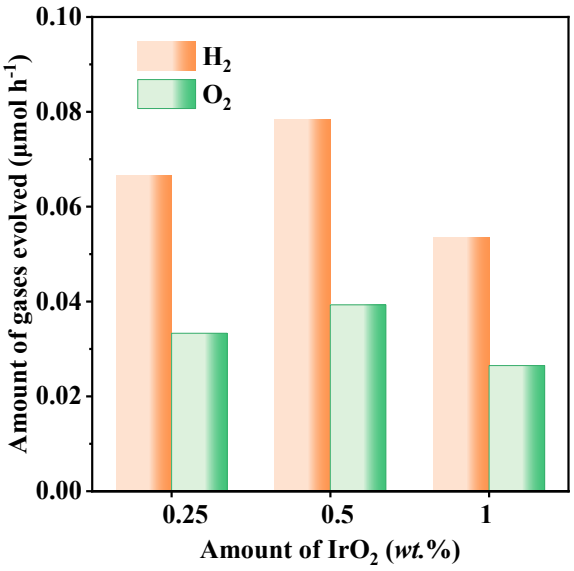

Fig. S7 Optimization loading content of IrO_2 cocatalyst on Pt@CrO_x/$YbTaO_{4-x}N_y$(Mg) for overall water splitting.

Reaction conditions: 100 mg photocatalyst, 150 mL H_2O, 300 W Xe lamp with a cutoff filter ($\lambda \geq 420$ nm).

References

1. F. Zhang, A. Yamakata, K. Maeda, Y. Moriya, T. Takata, J. Kubota, K. Teshima, S. Oishi and K. Domen, *J. Am. Chem. Soc.*, 2012, **134**, 8348-8351.
2. Y. Qi, J. Zhang, Y. Kong, Y. Zhao, S. Chen, D. Li, W. Liu, Y. Chen, T. Xie, J. Cui, C. Li, K. Domen and F. Zhang, *Nat. Commun.*, 2022, **13**, 484.
3. C. Le Paven-Thivet, A. Ishikawa, A. Ziani, L. Le Gendre, M. Yoshida, J. Kubota, F. Tessier and K. Doment, *J. Phys. Chem. C*, 2009, **113**, 6156-6162.
4. B. Toby, *J. Appl. Crystallogr.*, 2001, **34**, 210-213.